Ceramics International **24** (1998) 393–400

PII: S0272-8842(97)00027-8
0272-8842/98 $19.00+.00

Synthesis and Characterization of Ultrafine Zircon Powder

Ying Shi, Xiaoxian Huang & Dongsheng Yan

Shanghai Institute of Ceramics, Chinese Academy of Sciences, 1295 Dingxi Road, 200050 Shanghai, People's Republic of China

(Received 2 January 1997; accepted 17 April 1997)

Abstract: The synthesis of ultrafine zircon ($ZrSiO_4$) powder with high purity was studied by using $ZrOCl_2$ solution and fumed SiO_2 as starting materials. The zircon precursor gels which were obtained by a wet chemical precipitation were seeded with zircon sand powder. The influences of processing, seed content and calcination temperature on the synthesis of zircon powder were investigated by XRD, TEM and IR spectroscopy etc. It was found that the washing of seeded gels by ethanol greatly benefited the formation of zircon at lower temperatures. Single-phase zircon powder can be obtained from the precursor gel seeded by 3 mol% zircon sand particles when calcined at 1400°C for 2 h with primary particle size of 0.2–0.3 μm and impurities content of less than 0.2 wt%. The mechanism of zircon formation is heterogeneous nucleation due to the existence of zircon seeds. The relative density of hot-pressed sintered zircon at 1600°C for 1h reaches 99.1% theoretical and its flexural strength and fracture toughness at room temperature are 320 ± 15 MPa and 3.0 ± 0.4 MPa·m$^{1/2}$, respectively.

1 INTRODUCTION

Zircon ($ZrSiO_4$) is an important ceramic material because of its low coefficient of thermal expansion (about 4.1×10^{-6} °C^{-1} between 25°C and 1400°C) as well as its low coefficient of heat conductivity (5.1 W m^{-1} °C^{-1} at room temperature and 3.5 W m^{-1} °C at 1000°C).[1,2] It does not undergo any structural transformation until dissociation at about 1700°C according to the ZrO_2–SiO_2 system phase diagram. Sintered zircon bodies present a very high chemical stability, high resistance to melt corrosion, excellent thermal shock resistance and good high temperature mechanical properties, so it is widely applied in high temperature fields where sudden temperature changes are to be encountered. In recent years, more and more attention has been given to its applications as structural ceramics.[3] The impurities in natural zircon powder limit its applications, especially in high temperature conditions because the impurities not only deteriorate the high temperature mechanical properties seriously, but also decompose zircon at temperatures much lower than its normal melting point. For example, Al_2O_3 would react with zircon in the range of 1300°C–1400°C to form mullite and ZrO_2 as follows:

$$2ZrSiO_4 + 3Al_2O_3 = 3Al_2O_3.2SiO_2 + 2ZrO_2$$

So it is of great importance to synthesize ultrafine zircon powder with high chemical purity for more reliable application of zircon, especially at elevated temperatures.

Earlier studies have been performed on the preparation of zircon powders.[3–5] The process developed in these research works was generally by the sol–gel method, starting with zirconium oxychloride ($ZrOCl_2$) solution and tetraethoxysilane ($Si(C_2H_5O)_4$) or colloidal SiO_2 and resulted in almost single-phase zircon powder with impurities much less than natural zircon sand. Toshiyuki Mori synthesized highly pure single phase $ZrSiO_4$ fine powder via zircon precursors having a Zr–O–Si bond formed during hydrolysis at 100°C in a sol–gel process. The mean particle size was 0.5 μm

and the total impurity content was about 0.3 wt%, much less than natural zircon sands.[3] Other methods have also been reported, such as the spray thermal decomposition method and the hydrothermal process.[6,7]

In this paper, a new wet chemical process is developed to synthesize high-purity ultrafine zircon powder. Homogeneous gel precipitates were prepared by a wet chemical process, and a small amount of zircon sand seeds was mixed into the gels in order to promote the formation of zircon and lower the calcination temperature. The effects of seed contents and calcination temperature and other factors on the synthesis of zircon powder have been investigated. The formation mechanism of zircon powder has also been discussed. The obtained zircon powders were characterised by chemical analysis, TEM, XRD, and the mechanical properties of $ZrSiO_4$ sintered bodies were also determined.

2 EXPERIMENTAL PROCEDURE

$ZrOCl_2 \cdot 8H_2O$ and fumed silica were used as the starting materials. $ZrOCl_2 \cdot 8H_2O$ was dissolved in distilled water. The average particle size of fumed SiO_2 is about 20 nm and the content of impurities is less than 0.1 wt%. A homogeneous slurry was obtained after f-SiO_2 was mixed with the solution according to the molar ratio of Zr/Si = 1.0. The slurry was brought to pH = 10 by adding aqueous ammonia solution under vigorous stirring. The homogeneous gels obtained were filtered and washed with distilled water to pH = 7–8, and afterwards washed with ethanol. A small amount of zircon sand powder was thoroughly mixed with washed gels as seeds to foster zircon formation. The mixing of zircon seed was carried out by the means of wet ball-milling using ZrO_2 ball as media. The average particle size of seed powder was 1 μm and the total impurities content was 6–7 wt%. After drying at 120°C for 24 h, the mixtures were calcined at temperatures between 1000°C and 1450°C.

The formation rate of zircon (α_{ZR}) in the synthesized powder was determined by XRD method (D/max-ra, X-ray diffractometer, Rigaku, Japan) through the following equation: [2,3]

$$\alpha_{ZR} = I_{ZR(200)}/[I_{ZR(200)} + I_{m(1\bar{1}1)} + I_{m(111)} + I_{t(111)}] \quad (1)$$

where $I_{(ABC)}$ is the intensity of diffraction peak of (ABC) crystal plane, subscripts *ZR*, *m* and *t* stand for $ZrSiO_4$, m-ZrO_2 and t-ZrO_2, respectively. The four diffraction peaks in eqn (1) appeared at the diffraction angle 2θ in the range of 26°–32°.

The chemical compositions of synthesized powders were analysed by wet chemical method. Washed gels and obtained powders were examined by transmission electron microscopy (JEM-200CX, Japan), infrared spectrophotometry (Nicolet, model 7199C)). The specific surface area of the powder was measured by BET method (Quantachrome Co. model Autoaorb-I) while the average particle size (D_{50}) of the zircon powder (Brookhaven Co. model Bi-DCP1000) was determined also.

The synthesized zircon powder was hot-pressed in a graphite die at 1600°C for 1 h under 30 MPa in an inert atmosphere. The specimens were cut into 2.5×5×30 mm bars with a diamond wheel to measure flexural strength by the 3-point bending test with a span of 20 mm and a crosshead speed of 0.5 mm min^{-1}. Test bars of dimensions of 5×2.5×30 mm were prepared for single edge notch-beam (SENB) method to measure fracture toughness with a span of 20 mm and a crosshead speed of 0.05 mm min^{-1}. The notches used were 0.25 mm and 2.5 mm depth. All mechanical measurements were carried out on an Instron-1195 material tester. Sample density was measured using the Archimedes' method.

3 RESULTS AND DISCUSSION

3.1 Evaluation of precipitated gels

Figure 1 shows the TEM micrographs of precipitated gels obtained by different washing processes, gel-P was only washed by distilled water to pH = 7–8, while gel P-E was washed by ethanol for three times after being washed by distilled water (indicated in Table 1). It is obvious that two kinds of gel particles were composed of many small primary particles in nanometre scale. EDAX analysis of gel P-E indicates that gel particles contain Zr and Si equimolarly, so it is suggested that the precipitated gels consist of $Zr(OH)_4$ and fumed SiO_2 homogeneously for they were obtained from $ZrOCl_2$ solution in which fumed SiO_2 particles were well-dispersed according to the stoichiometric ratio of Zr/Si = 1. (A little excess of $ZrOCl_2$ solution was used to ensure no residual SiO_2 remained in the obtained zircon powder.) Furthermore, micrographs of gels show that gel P-E has a better state of agglomeration than gel P. After being washed by ethanol, the dried gel P-E was more soft and friable than gel P. The specific surface area of gel P-E is somewhat larger than that of gel P (Table 1).

IR spectra of gels (Fig. 2) showed that there was an absorption band in the vicinity of 3000 cm^{-1}, corresponding to C-H stretching absorption. This band shows the evidence of interaction of ethanol with the gel P. Absorption contributions from C-O stretching in ethanol cannot be observed because of overlap with silica bands at 1100–1000 cm^{-1}. Comparing two different washing routes, it is clear that the lower surface tension of ethanol ($\tau_{C2H5OH} = 22.8$ N m^{-2}) contrasted to water ($\tau_{H2O} = 72.8$ N m^{-2}) leads to lower capillary force and improves the agglomeration state in gel P, owing to the removal of non-bridging hydroxyl groups and co-ordinated water of gels, which had been proposed in the research work on the preparation of ultrafine zirconia powder.[3]

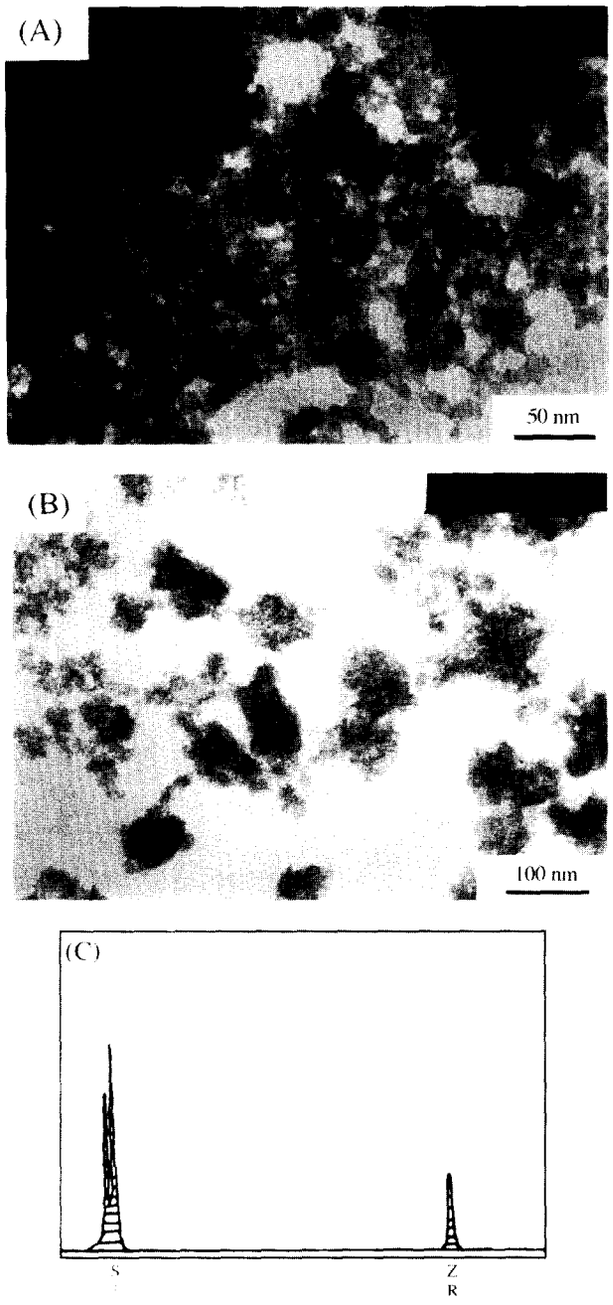

Fig. 1. TEM micrographs of precipitate gels washed by different solvents: (A) gel P; (B) gel P-E; (C) EDAX of gel P-E.

Table 1. Characterization of precipitate gels

Gel sample	Washing solvents	S_{BET} ($m^2 g^{-1}$)	Molar ratio of Zr/Si
P	H_2O	305	
P-E	H_2O and C_2H_5OH	351	1.03

3.2 Synthesis of ultrafine zircon powder

It was known that zircon powder could not be synthesized by solid-state reaction unless at a relatively high temperature (> 1500°C), but the content of zircon phase in the obtained powder was still not high, normally no more that 50%.[4] So mixing of natural zircon sand into precursor as seeds was attempted in our processing in order to promote the formation of zircon and lower the calcination temperature.

Figure 3 shows the relation between the formation rates of zircon (α_{ZR}) and the content of seeds in gel P-E under different calcination conditions.

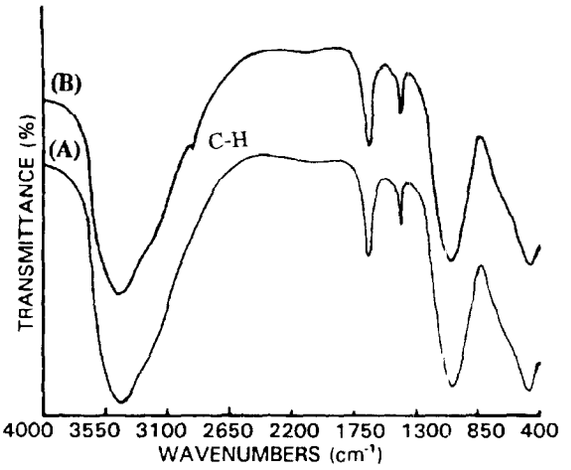

Fig. 2. IR spectra of precipitated gels: (A) gel P; (B) gel P-E.

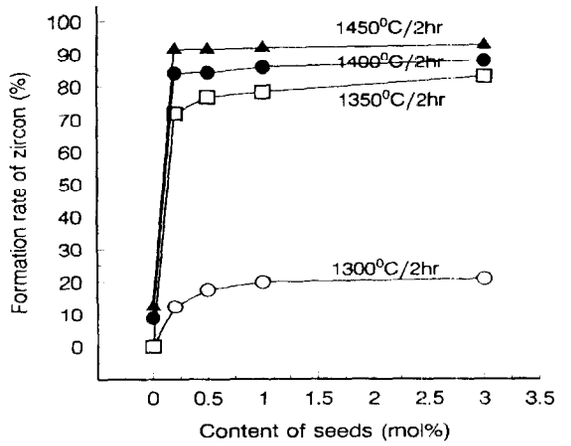

Fig. 3. The dependence of formation rate of zircon on the seed content at different calcination temperatures.

From the curves plotted, it may be concluded that calcination temperature and the content of seeds are the two crucial elements dominating zircon formation. At a calcination temperature of 1300°C, the formation rate of zircon is very low (below 30%), even though 3 mol% seeds were mixed into the gel. When the calcination temperature was raised above 1350°C, the seeds began to play a significant role in promoting zircon formation. With the addition of the first half per cent of seeds, the increase of α_{ZR} is most dramatic, but it levels off quickly at and beyond 1%. Under the same seed contents added, the effect on zircon formation with increasing temperature is also obvious as shown in Fig. 3. The formation rate of zircon in 3 mol% seeded gel P-E could reach 95% on the calcining conditions of 1450°C $2\,h^{-1}$.

Figure 4 displays the X-ray diffraction patterns of the gel P-E containing 3 mol% seeds calcined at different temperatures for 2 h, showing the dependence of reaction and compound formation with the calcination temperature. There is almost no zircon formed in gel P-E after calcination up to 1200°C for 2 h and t-ZrO_2 is the main phase appearing in the powder. However, when the calcination temperature was increased to 1300°C, the solid-state reaction between t-ZrO_2 and f-SiO_2 to form zircon became predominant and zircon appeared to be the major phase. After calcination at 1400°C for 2 h, a single phase zircon powder was obtained with a small diffraction peak of t-ZrO_2 owing to the little overdose of $ZrOCl_2$ in the starting composition. The infrared spectra of gel P-E (3 mol% seeded) calcined at various temperatures shown in Fig. 5 indicate the same results, the characteristic peaks of zircon (Zr–O–Si bond at 880 cm^{-1} and 640 cm^{-1}) are intensified as the calcination temperature increases, the pattern (D) in Fig. 5 (calcined at 1400°C for 2 h) is identical with the standard IR pattern of zircon.

Morphologies of the powder calcined at different temperatures under TEM are shown in Fig. 6. Considering the results of XRD (Fig. 5(B)), it may be suggested that the small particles in (A) of about 30–50 nm in size are t-ZrO_2, surrounded by amorphous fumed SiO_2. Two sets of diffraction patterns in Fig. 6(B) demonstrated that prior to the formation of zircon, $Zr(OH)_4$ in gel P-E has turned into polycrystalline t-ZrO_2 and fumed SiO_2 remains in the amorphous state, which was in good agreement with XRD results. Figure 6(C) and (D) showed that the formation of zircon

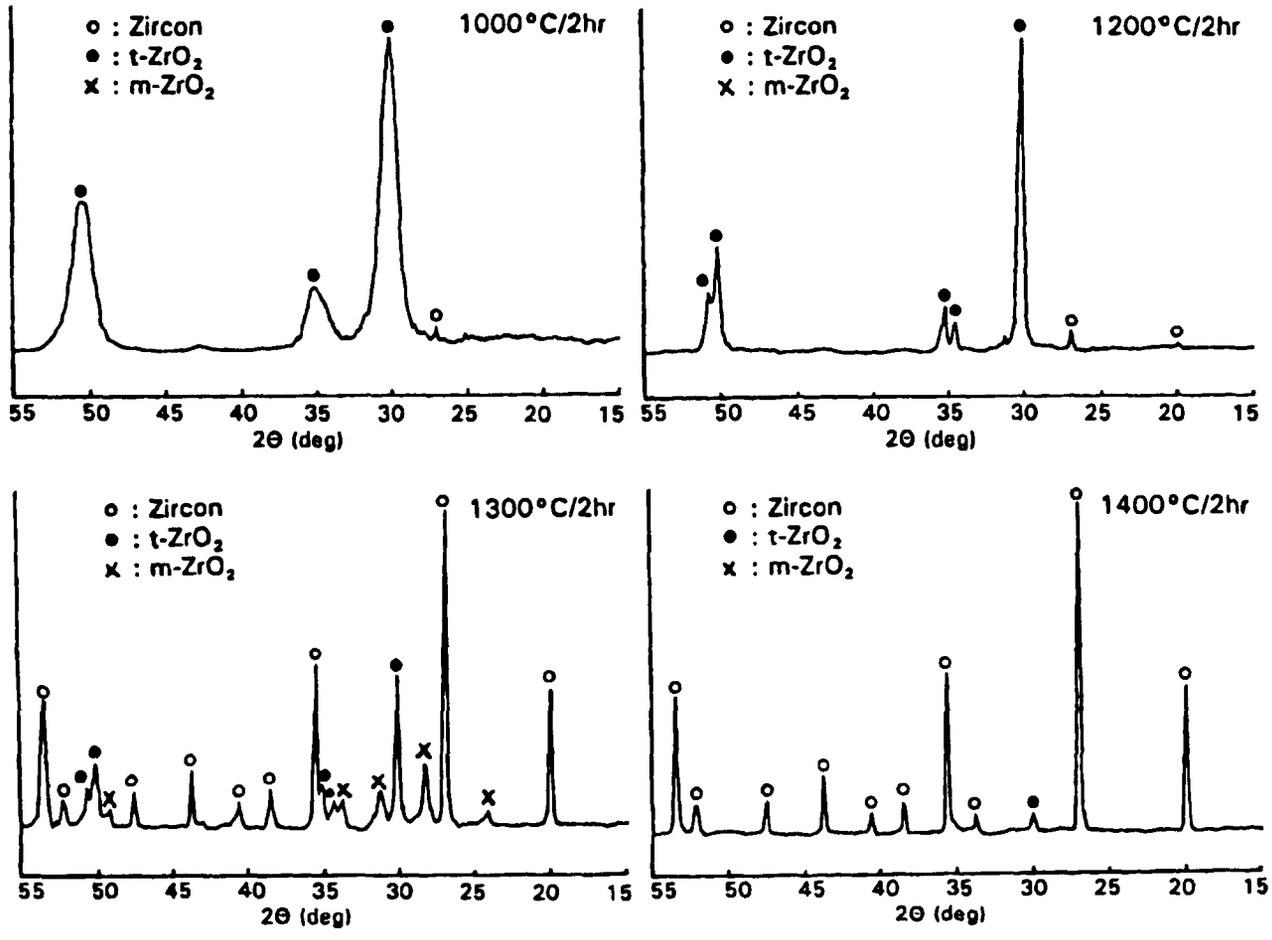

Fig. 4. X-ray diffraction patterns of gel P-E (3 mol% seeded) calcined at different temperatures.

occurs substantially when the calcining temperature was above 1300°C, which coincides with the results of XRD and IR patterns perfectly. So the reaction sequence for zircon formation can be traced as follows:

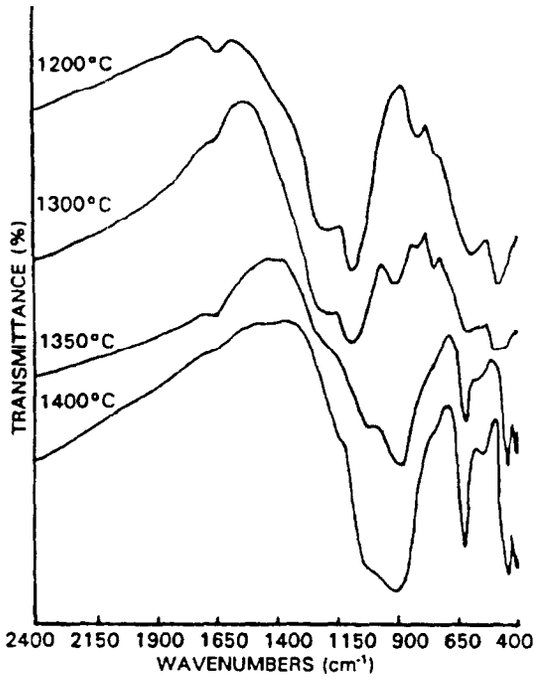

Fig. 5. IR spectra of gel P-E (3 mol% seeded) calcined at different temperatures.

$$\begin{array}{c} \text{Gel P-E}(Zr(OH)_4 + \text{fumed } SiO_2) \\ \downarrow \text{ below } 1200\ ^\circ C \\ t - ZrO_2 + \text{fumed } SiO_2 \\ \downarrow 1200\ ^\circ C - 1300\ ^\circ C \\ ZrSiO_4 + (t, m) - ZrO_2 + \text{fumed } SiO_2 \\ \downarrow 1400\ ^\circ C \\ ZrSiO_4 \end{array}$$

3.3 Formation mechanism of zircon

Due to the addition of zircon sand seeds in gel during the wet chemical process, a great deal of free surface was provided on which the new zircon nucleus would preferentially form by heterogeneous nucleation instead of homogeneous nucleation when there were no seeds in gel system. The surface energy of seeds decreased the thermodynamic barrier for zircon nucleation reaction greatly.[9] The extent to which the nucleation barrier could be lowered from its homogeneous value ΔG_{hom} when no seeds were existing depends entirely on the contact angle θ, representing the matching degree of crystal structure between seeds and newly formed phase. In our case, θ tends to be zero since the seeds phase and the synthesized phase are the same, so the energy barrier of heterogeneous nucleation:[10]

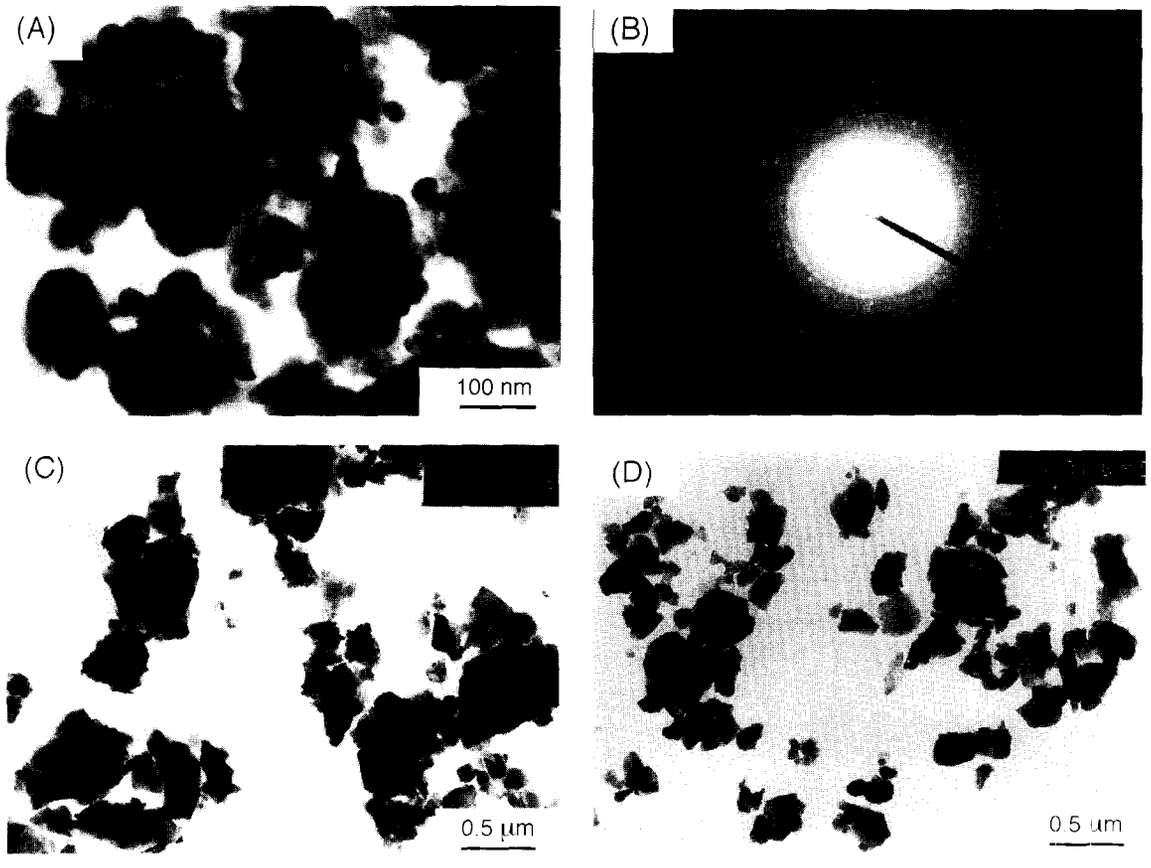

Fig. 6. TEM micrographs of gel P-E (3 mol% seeded) calcined at different temperatures: (A) 1200°C; (B) SAD image of (A); (C) 1300°C; (D) 1400°C.

$$\Delta G_{het} = \Delta G_{hom} \cdot (2 - 3\cos\theta + \cos^3\theta)/4 \qquad (2)$$

dropped conspicuously. Figure 7 shows the dependence of energy barriers associated with heterogeneous and homogeneous nucleation on nucleus radius. As a result, zircon nucleus formation was promoted remarkably at relatively lower temperatures. When the radius of a zircon nucleus newly formed on the surface of seeds exceeded the critical nucleus size r*, it could exist stably in the reaction system and grow further. Figure 8(A) shows the morphology of zircon sand seed which was surrounded by homogeneous gel in gel P-E (3 mol% seeded) before calcination, while Fig. 8(B) displays the morphology of small zircon particles newly formed on the seed surface, proving the validity of heterogeneous nucleation.

3.4 Dynamic analysis of zircon formation

Figure 9 shows the corresponding formation rates of zircon in gel P-E and P (3 mol% seeded) with increasing holding time isothermally heated at 1300°C. It is observed that the rate of zircon formation in gel P-E is significantly higher than that in gel P and the α_{ZR} value increases at a faster rate with holding time. Therefore, it seems that the formation of zircon could be fostered in the process by employing ethanol washing of the gel.

In general, the formation rate of newly formed phase (X) in a given solid state transformation can be expressed as:[11]

$$X = 1 - \mathrm{EXP}(-K^n \cdot t^n) \qquad (3)$$

where K is the reaction rate constant, t is the holding time, and n is the time exponent relating to

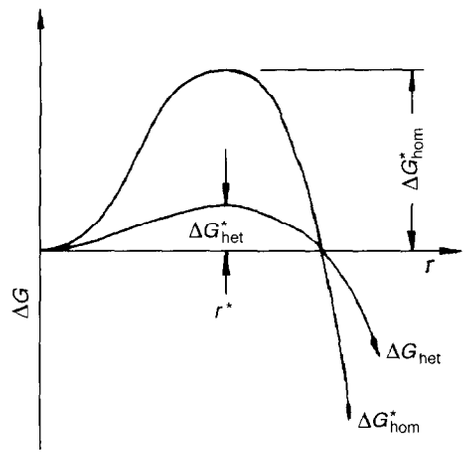

Fig. 7. The dependence of energy barriers associated with homogeneous and heterogeneous nucleation on nucleus radius.

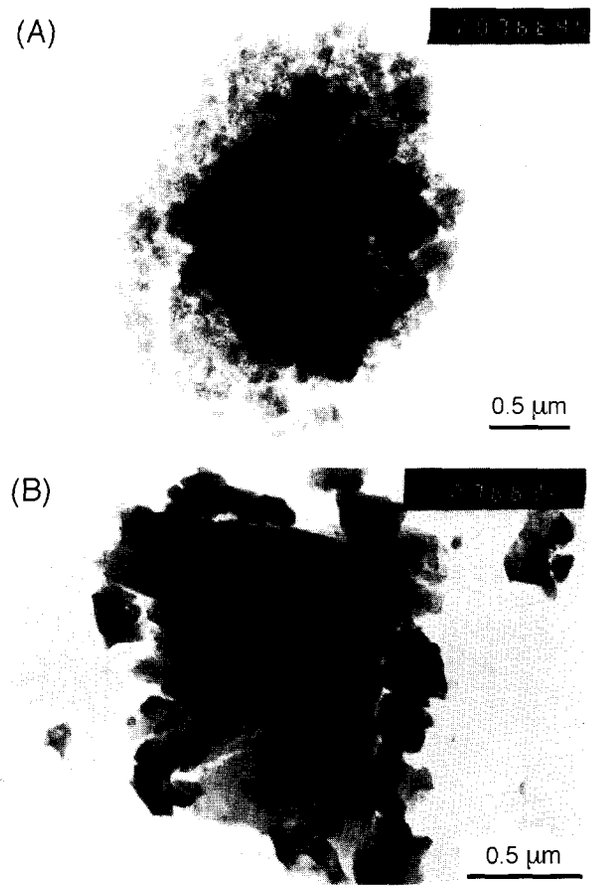

Fig. 8. The morphology of zircon seed in the precipitated gel P-E: (A) before calcination; (B) calcined at 1400°C for 2 h.

the different reaction mechanisms. When the formation rate of new phase is controlled by diffusion, the transformation fraction can be written as [12]

$$\ln(\ln(1 - X)^{-1}) = 3/2 \cdot \ln t + C \qquad (4)$$

C is a constant for a given temperature. The kinetics of zircon formation in gel P and gel P-E were analysed by using the data of Fig. 9 according to eqn (4). A plot of $ln[ln(1 - \alpha_{ZR})^{-1}]$ with respect to

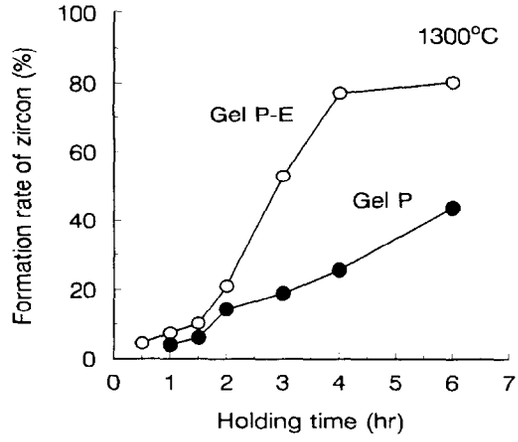

Fig. 9. The relationship of formation rate of zircon in the gel P-E and P (3 mol% seeded) with holding time at 1300°C.

ln t gives two relevant straight lines as shown in Fig. 10, with slopes being close to 3/2 approximately. Therefore, it may be argued that the zircon formation reaction seems to be a diffusion-controlled process rather than an interfacial reaction-controlled one, the overall reaction rate is actually controlled by the diffusion process under fast nucleation (Avrami regime).[11]

3.5 Characteristics of the synthesized zircon powder

Summarizing the results obtained above, zircon powders were synthesized under the conditions described as follows: seeded 3 mol% zircon sand in the precipitate gel and calcined at 1400°C for 2 h.

The chemical compositions of the seeds and the synthesized zircon powder are listed in Table 2. Comparing with natural zircon sand, the synthesized powder has a lesser amount of impurities, about 0.153 wt% in total which were mainly brought in by the adding of 3 mol% seeds.

The particle size of zircon powder obtained was determined by several methods. TEM observation (Fig. 11) shows that the synthesized ultrafine zircon powders are composed of uniform submicrometer particles. The primary particle size of powder P-E (Fig. 11(B)) is about 0.2–0.3 μm, which is finer than that of powder P (Fig. 11(A)), and the state of agglomeration is more insignificant. In Table 3, particle sizes determined by specific surface area method (D_{BET}) and particle size distribution (D_{50}) were compared for synthetic powder P and P-E, as well as seed powder used in our processing.. The specific surface area and average particle size by BET method are 4.9 $m^2\ g^{-1}$ and 0.27 μm for powder P, 5.2 $m^2\ g^{-1}$ and 0.25 μm for powder P-E, respectively, which are in general agreement with the primary particle size determined by TEM observation.

Synthesized zircon powder P-E was hot-pressed at 1600°C for 1 h in an inert atmosphere under a pressure of 30 MPa. The bulk density of the specimens reaches 4.63 g cm^{-3}, which is about 99.1% theoretical (4.67 g cm^{-3} for the theoretical density of zircon). The flexural strength and the fracture toughness at room temperature are 320 ± 15 MPa and 3.0 ± 0.5 MPa·$m^{1/2}$, respectively.

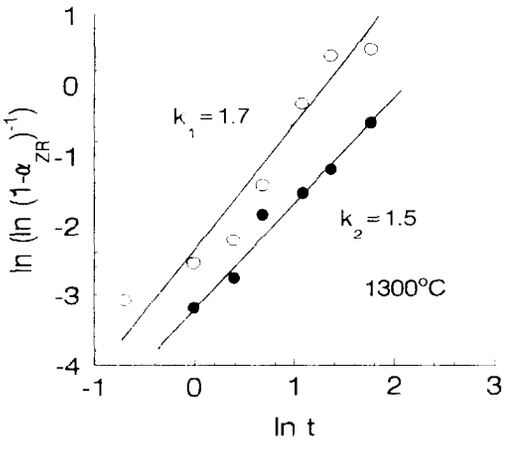

Fig. 10. The Avrami-type plot for formation of zircon in gel P-E and P (3 mol% seeded) calcined at 1300°C.

Table 2. The chemical compositions of the zircon seed and the synthesized powder

Composition	Synthesized powder (wt%)	Seed powder (wt%)
ZrO_2	67.22	62.28
SiO_2	30.85	31.17
HfO_2	1.39	1.26
Al_2O_3	0.11	3.17
Fe_2O_3	0.029	0.14
TiO_2		0.44
MgO	0.014	0.081
CaO		0.27
Y_2O_3		0.11

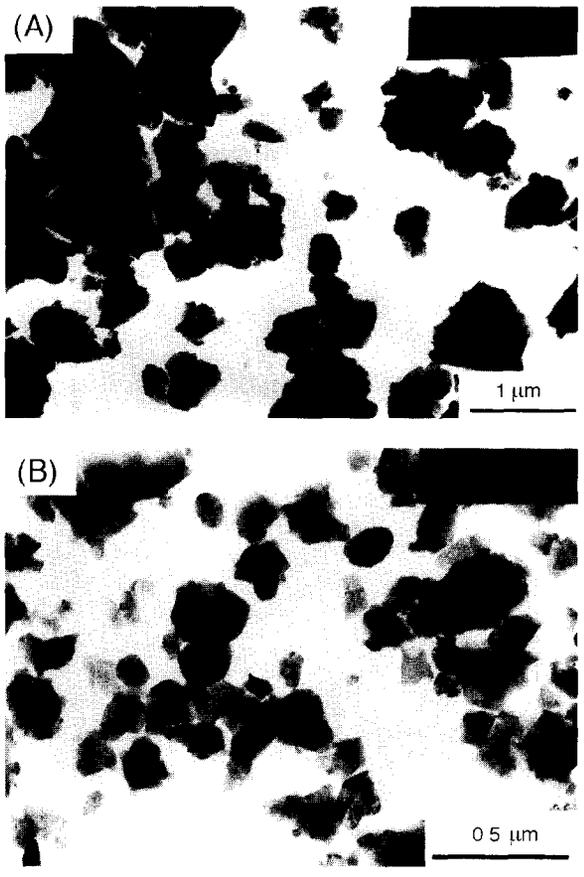

Fig. 11. TEM micrographs of synthesized ultrafine zircon powders (1400°C 2 h^{-1}): (A) powder P; and (B) powder P-E.

Table 3. A comparison of specific area and particle size for different zircon powder

	Powder P-E	Powder P	Seed
S_{BET} ($m^2\ g^{-1}$)	5.2	4.9	3.5
D_{BET} (μm)	0.25	0.27	0.37
D_{50} (μm)	0.85	1.26	1.32

4 CONCLUSIONS

1. Highly pure ultrafine zircon powders were prepared by wet chemical process using $ZrOCl_2$ and fumed SiO_2 as starting materials. From the results of our study, the best conditions for the synthesis of zircon are: a precipitated gel seeded with 3 mol% zircon sand particles and calcined at 1400°C for 2 h.
2. Addition of zircon seeds even at very low weight percentages, has a remarkably favourable affect on the synthesis of zircon with a lowering of formation temperature. The effect can be explained by heterogeneous nucleation on the seed surface leading to the decrease of energy barrier for the zircon formation reaction, which appears to be diffusion-controlled judging by the data obtained from reaction kinetics.
3. The ultrafine zircon powder obtained is uniform 0.2–0.3 μm in average grain size.The total impurity content is less than 0.2 wt%. It also exhibits good sinterability and mechanical properties. For a specimen hot-pressed at 1600°C for 1 h under the pressure of 30 MPa, its relative density reaches 99.1% and its flexural strength and fracture toughness amount to 320 ± 15 MPa and 3.0 ± 0.4 MPa·$m^{1/2}$, respectively.

REFERENCES

1. SINGH, R. N., *J. Am. Ceram. Soc.*, **73** (1990) 2399.
2. MORI, T., HOSHINO, H., ISHIKAWA, Y., YAMAGUCHI, T., YAMAMURA, H., KOBAYASHI, H. & MITAMURA, T., *J. Ceram. Soc. Jap.*, **99** (1991) 227.
3. MORI, T., YAMAMURA, H., KOBAYASHI, H. & MITAMURA, T., *J. Am. Ceram. Soc.*, **75** (1992) 2420.
4. HAAKER, R. F. & EWING, R. C., *Commun. Am. Ceram. Soc.*, (1981) C-149.
5. VILMIN, G., KOMANRENI, S. & ROY, R., *J. Mater. Sci.*, **22** (1987) 3556.
6. JADA, S. S., *J. Mater. Sci. Lett.*, **9** (1990) 565.
7. KIMARNENI, S. & ROY, R., *Zircon Science and Technology*, ed. S. Somiya, 1988, pp. 289–298.
8. KALISZEWSKI, M. S. & HEUER, A. H., *J. Am. Ceram. Soc.*, **73** (1990) 1504.
9. SHI, Y., HUANG, X. X. & YAN, D. S., *Mater. Lett.*, **21** (1994) 79.
10. KINGERY, W. D., BOWEN, H. K. & UHLMANN, D. R., *Introduction to Ceramics*, 2nd edn. John Wiley & Sons, New York, 1976, pp. 334–335.
11. LIM, B. C. & JANG, H. M., *J. Am. Ceram. Soc.*, **76** (1993) 1482.
12. RAGHAVEN, V. & COHEN, M., *Treatise on Solid State Chemistry*, ed. N. B. Hannay. Plenum Press, New York, 1982, pp. 67–127.